

Maximum Entropy-Based Interference-plus-Noise Covariance Matrix Reconstruction for Robust Adaptive Beamforming

Saeed Mohammadzadeh[†], Vítor H. Nascimento[†], Rodrigo C. de Lamare^{††} and Osman Kukrer^{†††}

Abstract—To ensure signal receiving quality, robust adaptive beamforming (RAB) is of vital importance in modern communications. In this letter, we propose a new low-complexity RAB approach based on interference-plus-noise covariance matrix (IPNC) reconstruction and steering vector (SV) estimation. In this method, the IPNC and desired signal covariance matrices are reconstructed by estimating all interference powers as well as the desired signal power using the principle of maximum entropy power spectrum (MEPS). Numerical simulations demonstrate that the proposed method can provide superior performance to several previously proposed beamformers.

Index Terms—Covariance matrix reconstruction, Maximum entropy method, Robust adaptive beamforming, Spatial power spectrum.

I. INTRODUCTION

ADAPTIVE beamforming has been intensively developed for spatial filtering with applications in wireless communications, radar and microphone array processing [1]. However, adaptive beamformers may suffer performance degradation due to several reasons, which include short data records, the presence of the signal-of-interest (SOI) in the training data, or imprecise knowledge of the steering vector (SV) of the desired signal [2]–[4]. Hence, various techniques have been developed to improve the performance of adaptive beamformers in the presence of mismatches. These robust adaptive beamforming (RAB) techniques can be divided into the following types: diagonal loading approaches [5], [6], the eigenspace-based beamformer [7], [8], worst-case optimization and SV estimation with presumed prior knowledge [9]–[11], and estimation of the mismatched SV using Sequential Quadratic Programming (SQP) [12]. However, RAB designs based on these approaches have some drawbacks such as their ad hoc nature, high probability of subspace swap at low signal-to-noise ratio (SNR) and high computational complexity.

Recently, a new approach to RAB was presented that removes the influence of the SOI component from the sample covariance matrix by reconstructing the interference-plus-noise-covariance (IPNC) matrix [13]–[19]. The IPNC matrix in [13] is reconstructed based on the Capon spectral estimator by integrating over an angular sector that excludes the direction-of-arrival (DoA) of the SOI. In [14], a computationally efficient algorithm via low complexity shrinkage-based mismatch estimation (LOCSME) is proposed followed by the

introduction of the orthogonal Krylov subspace projection mismatch estimation (OKSPME) technique [20]. The approach in [15] makes use of prior information about the angular sections of the signals and combines projection methods to obtain more precise estimates of the IPNC matrix, but its performance degrades with the increase of the number of interferers. Later, in [16] an algorithm is developed using spatial power spectrum sampling (SPSS), which has lower computational complexity, but its performance is degraded as the number of sensors is decreased. In [18] a procedure analogous to those of [13] and [3] is used to reconstruct the IPNC matrix and to estimate the desired signal SV. However, the accuracy of the interference SV estimate is sensitive to the value of an ad hoc parameter. The results of [13] indicate that the resulting Capon beamformer achieves better performance in the case of SOI array SV errors compared to the previous approaches. However, the analysis in [13] did not account for typically present interference array SV errors or arbitrary SOI array SV mismatches [21]. Moreover, the accuracy of the Capon spatial spectrum degrades severely when coherent signals (with line spectra) exist [22].

The main contribution of this paper is to develop a novel RAB approach that achieves nearly optimal performance by addressing the inaccurate covariance matrix construction problem as well as errors due to DoA mismatches and other array imperfections. The idea is based on IPNC matrix reconstruction and the desired signal SV estimation using maximum entropy power spectrum (MEPS), a method that, although available for a long time, was not yet applied to beamforming. In contrast to prior work with IPNC, we apply MEPS to reconstruct the IPNC matrix by integrating over the angular sector of interference-plus-noise as well as the desired signal region. Then, a desired signal SV estimate is introduced to replace the SOI's presumed SV. The proposed approach outperforms existing techniques with less computational complexity.

II. PROBLEM BACKGROUND

Consider a uniform linear antenna array (ULA) of M isotropic sensors spaced by distance d receiving signals from far-field narrowband sources. The array observation vector at time t can be modeled as

$$\mathbf{x}(t) = s(t)\mathbf{a}(\theta_s) + \mathbf{i}(t) + \mathbf{n}(t), \quad (1)$$

where the signals $x_l(t)$ observed at each antenna are collected in the vector $\mathbf{x}(t) = [x_0(t) \dots x_{M-1}(t)]^T$, and $(\cdot)^T$ is the transpose while $\mathbf{i}(t)$, $\mathbf{n}(t)$, $s(t)$ denote the components of the

[†]Dept. of Electronic Systems Engineering, Univ. of São Paulo, Brazil. ^{††}CETUC, PUC-Rio, Brazil. ^{†††}Eastern Mediterranean Univ., Turkey. This work was partially funded by Fapesp through the ELIOT project, grants 2018/12579-7 and 2019/19387-9.

interference, the zero-mean Gaussian noise vector and the waveform of the SOI, respectively. For a ULA with M sensors the SV corresponding to the DoA of the SOI is

$$\mathbf{a} = \mathbf{a}(\theta_s) = \left[1, e^{-j2\pi\bar{d}\sin\theta_s}, \dots, e^{-j2\pi(M-1)\bar{d}\sin\theta_s} \right]^T, \quad (2)$$

where $\bar{d} = d/\lambda$, λ is the wavelength. Assuming that the SV \mathbf{a} is known, then for a given beamformer weight vector \mathbf{w} , the beamformer's performance is measured using the output signal-to-interference-plus-noise ratio (SINR) as follows

$$\text{SINR} = \frac{\sigma_s^2 |\mathbf{w}^H \mathbf{a}|^2}{\mathbf{w}^H \mathbf{R}_{i+n} \mathbf{w}}, \quad (3)$$

where σ_s^2 is the desired signal power, $\mathbf{R}_{i+n} = \mathbb{E}\{(\mathbf{i}(t) + \mathbf{n}(t))(\mathbf{i}(t) + \mathbf{n}(t))^H\} \in \mathcal{C}^{M \times M}$ is the IPNC matrix, $\mathbb{E}\{\cdot\}$ denotes statistical expectation and $(\cdot)^H$ stands for Hermitian transpose. In order to achieve the maximum SINR, the interference-plus-noise output power is minimized while maintaining a distortionless response for the desired signal,

$$\min_{\mathbf{w}} \mathbf{w}^H \mathbf{R}_{i+n} \mathbf{w} \quad \text{s.t.} \quad \mathbf{w}^H \mathbf{a} = 1. \quad (4)$$

The solution to (4) yields the optimal beamformer given by

$$\mathbf{w}_{\text{opt}} = \frac{\mathbf{R}_{i+n}^{-1} \mathbf{a}}{\mathbf{a}^H \mathbf{R}_{i+n}^{-1} \mathbf{a}}. \quad (5)$$

Moreover, the theoretical array covariance matrix is denoted as $\mathbf{R} = \mathbf{R}_s + \mathbf{R}_{i+n}$, where $\mathbf{R}_s = \sigma_s^2 \mathbf{a} \mathbf{a}^H$ is the theoretical desired signal covariance matrix. This relation and the constraint $\mathbf{w}^H \mathbf{a} = 1$ imply that \mathbf{R}_{i+n} can be substituted by \mathbf{R} in (4) and (5) without changing the final result [1]. Since in practice, the exact IPNC matrix, \mathbf{R}_{i+n} and array covariance matrix, \mathbf{R} are unavailable even in signal-free applications, they are replaced by the sample covariance matrix $\hat{\mathbf{R}} = (1/K) \sum_{t=1}^K \mathbf{x}(t) \mathbf{x}^H(t)$, where K is the number of snapshots.

Both the direction of the SOI and the SV for a given direction are known imperfectly, due to errors in estimating θ_s and on positioning and calibration of the sensor array.

III. THE PROPOSED MEPS-IPNC ALGORITHM

Our approach is based on MEPS to reconstruct the interference-plus-noise covariance (MEPS-IPNC) matrix. We develop a procedure to reconstruct the IPNC matrix and then devise a low-complexity approach to estimate the actual SV.

A. Interference-plus-noise covariance matrix reconstruction

One of the limitations of the classical approach to spectrum estimation is that, for an observation vector of length M , the autocorrelation sequence can only be estimated for displacements $|k| < M$. Thus, it is set to zero for $|k| \geq M$. Since many signals of interest have autocorrelation that is nonzero for $|k| \geq M$, this windowing may significantly limit the accuracy of the estimated spectrum and resolution. This is particularly true in the case of narrowband processes that have autocorrelation that decays slowly with k .

Given the autocorrelation $r_x(k) = \mathbb{E}\{x_l(t)x_{l+k}(t)\}$ of a spatially stationary process for displacements $|k| \leq p$, the problem that we wish to address is how to extrapolate $r_x(k)$

for $|k| > p = M - 1$. Denoting the extrapolated values by $r_e(k)$, we can express the power spectrum in terms of the spatial frequency ν as follows

$$P_x(\nu) = \sum_{k=-p}^p r_x(k) e^{-jk\nu} + \sum_{|k|>p} r_e(k) e^{-jk\nu}. \quad (6)$$

It is clear that $P_x(\nu)$ should be real and non-negative for all ν . However, these constraints are not sufficient to guarantee a unique extrapolation. Therefore, [23] proposes to perform the extrapolation in such a way as to maximize the entropy of the process. Since entropy is a measure of uncertainty, a maximum entropy extrapolation is equivalent to finding the autocorrelation sequence, $r_e(k)$, that makes $\mathbf{x}(t)$ as white as possible. For a Gaussian random process with power spectrum $P_x(\nu)$, the entropy is [24]

$$H(\mathbf{x}) = \frac{1}{2\pi} \int_{-\pi}^{\pi} \ln P_x(\nu) d\nu. \quad (7)$$

Therefore, the MEPS of $r_x(k)$ is the one that maximizes (7) subject to the constraint that the inverse discrete time Fourier transform (IDTFT) of $P_x(\nu)$ equals the given set of autocorrelations for $|k| \leq p$

$$r_x(k) = \frac{1}{2\pi} \int_{-\pi}^{\pi} P_x(\nu) e^{jk\nu} d\nu; \quad |k| \leq p, \quad (8)$$

and the values of $r_e(k)$ may be found by

$$\frac{\partial H(\mathbf{x})}{\partial r_e^*(k)} = \frac{1}{2\pi} \int_{-\pi}^{\pi} \frac{1}{P_x(\nu)} \cdot \frac{\partial P_x(\nu)}{\partial r_e^*(k)} d\nu = 0; \quad |k| > p. \quad (9)$$

From (6) we see that

$$\frac{\partial P_x(\nu)}{\partial r_e^*(k)} = e^{jk\nu}, \quad (10)$$

which, when substituted into Eq.(9), yields

$$\frac{1}{2\pi} \int_{-\pi}^{\pi} \frac{1}{P_x(\nu)} e^{jk\nu} d\nu = 0; \quad |k| > p. \quad (11)$$

Defining $Q_x(\nu) = 1/P_x(\nu)$, (11) states that the IDTFT of $Q_x(\nu)$ is a finite-length sequence, equal to zero for $|k| > p$,

$$q_x(k) = \frac{1}{2\pi} \int_{-\pi}^{\pi} Q_x(\nu) e^{jk\nu} d\nu = 0; \quad |k| > p, \quad (12)$$

Therefore,

$$Q_x(\nu) = \frac{1}{P_x(\nu)} = \sum_{k=-p}^p q_x(k) e^{-jk\nu}, \quad (13)$$

and it follows that MEPS is an all-pole power spectrum

$$\hat{P}_{\text{meps}}(\nu) = \frac{1}{\sum_{k=-p}^p q_x(k) e^{-jk\nu}}. \quad (14)$$

Using the spectral factorization theorem [25], it follows that

$$\hat{P}_{\text{meps}} = \frac{|b(0)|^2}{C_p(e^{j\nu}) C_p^H(e^{j\nu})} = \frac{|b(0)|^2}{\left| 1 + \sum_{k=1}^p c_p(k) e^{-jk\nu} \right|^2}, \quad (15)$$

where $C_p(e^{j\nu}) = 1 + \sum_{k=1}^p c_p(k)e^{-jk\nu}$. Alternatively, in terms of the vectors $\mathbf{c}_p = [1, c_p(1), \dots, c_p(p)]^T$ and $\mathbf{e} = [1, e^{j\nu}, \dots, e^{jp\nu}]^T$, MEPS may be written as

$$\hat{P}_{\text{meps}} = \frac{|b(0)|^2}{|\mathbf{e}^H \mathbf{c}_p|^2}. \quad (16)$$

Having determined the form of MEPS, we must find the coefficients $b(0)$ and $c_p(k)$. Due to the constraint given in Eq. (8), these coefficients must be chosen in such a way that the IDTFT of \hat{P}_{meps} produces an autocorrelation sequence that matches the given values of $r_x(k)$ for $|k| \leq p$.

Therefore, it can be easily shown that the coefficients $c_p(k)$ are the solution to the autocorrelation normal equations [26]

$$\begin{bmatrix} r_x(0) & r_x^*(1) & \cdots & r_x^*(p) \\ r_x(1) & r_x(0) & \cdots & r_x^*(p-1) \\ \vdots & \vdots & \ddots & \vdots \\ r_x(p) & r_x(p-1) & \cdots & r_x(0) \end{bmatrix} \begin{bmatrix} 1 \\ c_p(1) \\ \vdots \\ c_p(p) \end{bmatrix} = \epsilon_p \begin{bmatrix} 1 \\ 0 \\ \vdots \\ 0 \end{bmatrix},$$

where $\epsilon_p = |b(0)|^2$. Therefore this equation is equivalent to

$$\hat{\mathbf{R}}\mathbf{c}_p = \epsilon_p \mathbf{u}_1 \Rightarrow \mathbf{c}_p = \epsilon_p \hat{\mathbf{R}}^{-1} \mathbf{u}_1, \quad (17)$$

where $\mathbf{u}_1 = [1 \ 0 \ \dots \ 0]^T$ and since $\mathbf{u}_1^T \mathbf{c}_p = 1$, it follows that $\epsilon_p = 1/\mathbf{u}_1^T \hat{\mathbf{R}}^{-1} \mathbf{u}_1$. Letting $\nu = 2\pi d \sin \theta$ implies $\mathbf{e} = \mathbf{a}(\theta)$, and the power spectrum estimate of maximum entropy is

$$\hat{P}_{\text{meps}} = \frac{1}{\epsilon_p (\mathbf{a}^H(\theta) \hat{\mathbf{R}}^{-1} \mathbf{u}_1 \mathbf{u}_1^H \hat{\mathbf{R}}^{-H} \mathbf{a}(\theta))}. \quad (18)$$

In order to find the MEPS-IPNC matrix, it is assumed that $\bar{\Theta} \subset [-\pi, \pi]$ is a set which contains the interference-plus-noise region and likewise the desired signal is located in the angular sector Θ , which can be obtained using low resolution direction finding methods. Exploiting the MEPS estimate (18), the IPNC matrix can be reconstructed by numerically evaluating

$$\hat{\mathbf{R}}_{\text{ipn}} = \int_{\bar{\Theta}} \hat{P}_{\text{meps}} \mathbf{a}(\theta) \mathbf{a}^H(\theta) d\theta. \quad (19)$$

Sampling $\bar{\Theta}$ uniformly with $L = \alpha M$ sampling points spaced by $\Delta\theta$ (our simulations show that $\alpha \approx 5$ is enough), (19) can be approximated by

$$\hat{\mathbf{R}}_{\text{ipn}} \approx \sum_{i=1}^L \frac{\mathbf{a}(\theta_i) \mathbf{a}^H(\theta_i)}{\epsilon_p (\mathbf{a}^H(\theta_i) \hat{\mathbf{R}}^{-1} \mathbf{u}_1 \mathbf{u}_1^H \hat{\mathbf{R}}^{-H} \mathbf{a}(\theta_i))} \Delta\theta. \quad (20)$$

B. Desired Signal Steering Vector Estimation

The focus of some recent adaptive beamforming methods is on using Capon spectral estimation to compute the power from the direction of the signal, which has some disadvantages. Let \mathbf{a} be the true SV for the SOI, and $\bar{\mathbf{a}}$ be the presumed one. The Capon spatial spectrum estimator [27] using the true SV, $1/\mathbf{a}^H \hat{\mathbf{R}}^{-1} \mathbf{a}$, can be approximated as the power of SOI-plus-noise. Since the Capon estimator has good resolution in spectrum estimation, $1/\bar{\mathbf{a}}^H \hat{\mathbf{R}}^{-1} \bar{\mathbf{a}}$ will deviate from $1/\mathbf{a}^H \hat{\mathbf{R}}^{-1} \mathbf{a}$ as long as mismatches between \mathbf{a} and $\bar{\mathbf{a}}$ occur. If the mismatch is large enough, $1/\bar{\mathbf{a}}^H \hat{\mathbf{R}}^{-1} \bar{\mathbf{a}}$ can be approximated as the power of noise only.

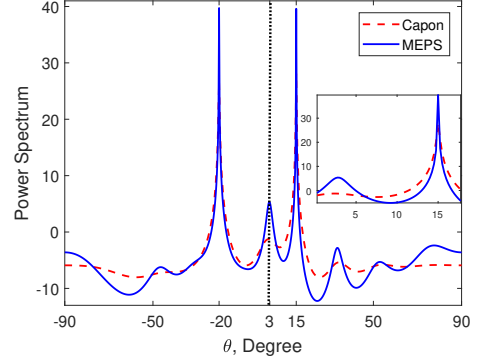


Fig. 1. Power spectrum of MEPS versus Capon estimators.

In practice, it is difficult to obtain the actual SV by simply using the presumed DoA of the signal because of propagation effects. Hence, the desired signal covariance matrix is reconstructed based on MEPS by numerically evaluating

$$\hat{\mathbf{R}}_s \approx \sum_{i=1}^S \frac{\mathbf{a}(\theta_{s_i}) \mathbf{a}^H(\theta_{s_i})}{\epsilon_p (\mathbf{a}^H(\theta_{s_i}) \hat{\mathbf{R}}^{-1} \mathbf{u}_1 \mathbf{u}_1^H \hat{\mathbf{R}}^{-H} \mathbf{a}(\theta_{s_i}))} \Delta\theta_s, \quad (21)$$

where now we sampled Θ uniformly with S sampling points spaced by $\Delta\theta_s$, so that $\{\mathbf{a}(\theta_{s_i}) | \theta_{s_i} \in \Theta\}$ lies within the range space of $\hat{\mathbf{R}}_s$. Note that in practice S can be chosen to be less than M , since Θ is usually a small sector. To improve the estimation accuracy of the desired signal SV, we propose a low-complexity algorithm to correct the presumed SV based on the fact that the product of the desired signal covariance matrix by any vector yields a vector proportional to the desired signal's SV. Hence, we can obtain an improved estimate for the desired signal SV as

$$\hat{\mathbf{a}} = \hat{\mathbf{R}}_s \bar{\mathbf{a}} \simeq (\sigma_s^2 \mathbf{a} \mathbf{a}^H) \bar{\mathbf{a}} \simeq \sigma_s^2 (\mathbf{a}^H \bar{\mathbf{a}}) \mathbf{a}, \quad (22)$$

which is proportional to the desired signal's SV provided that $\bar{\mathbf{a}}$ is not orthogonal to \mathbf{a} . Note that the proposed estimated array SV is accurate in the case of large look direction errors as well as random SV mismatches and local scattering imperfections as long as the choice of Θ separates well the desired signal and the interference regions, since (22) corresponds to one step of the power method [28]. Finally, we obtain the robust beamformer by substituting the reconstructed IPNC matrix, (19), and estimated desired SV, (22), back into (5) as follows

$$\mathbf{w}_{\text{prop}} = \frac{\hat{\mathbf{R}}_{\text{ipn}}^{-1} \hat{\mathbf{a}}}{\hat{\mathbf{a}}^H \hat{\mathbf{R}}_{\text{ipn}}^{-1} \hat{\mathbf{a}}}. \quad (23)$$

The computational complexity of MEPS-IPNC is $\mathcal{O}(M^2 L)$, where L is a small multiple of M . The solution of the QCQP problem in [13] to obtain the optimal weight vector has complexity of at least $\mathcal{O}(M^{3.5})$, while the beamformer in [7] has a complexity of $\mathcal{O}(KM) + \mathcal{O}(M^3)$ and the reconstructed IPNC matrices in [14] and [16] have a complexity of $\mathcal{O}(M^3)$ (in the latter cases, because the eigenvalue decomposition of $\hat{\mathbf{R}}$ is used.) However, their performance is significantly worse than that of MEPS-IPNC, as shown in the next section. Also, the cost of the beamformer in [18] is $\mathcal{O}(\max(M^2 S, M^{3.5}))$. Note that the complexity of MEPS-IPNC is similar to that of

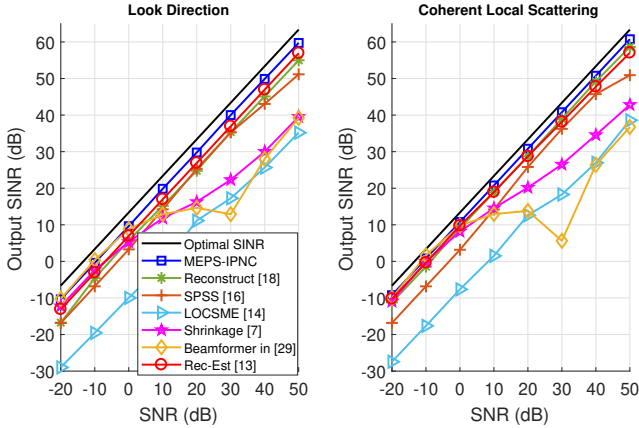


Fig. 2. SINR vs SNR a) Look Direction b) Coherent Local Scattering

the other methods for computing $\hat{\mathbf{R}}_{\text{ipn}}$, but the complexity for computing $\hat{\mathbf{a}}$ is smaller, since that depends on $S < M$ and on a single matrix-vector multiplication.

IV. SIMULATIONS

In this section, a ULA with $M = 22$ omnidirectional sensors is used. The additive noise is modeled as spatially white Gaussian with zero mean and unit variance. The angles of incidence of the desired signal and two interfering sources are $\bar{\theta}_s = 3^\circ, -20^\circ$ and 15° respectively. The input interference to noise ratios (INRs) of the two interferers are both set to 30 dB. We employ $L = 100, S = 20$, fixed SNR at 20 dB and $K = 30$ snapshots, and perform 100 Monte-Carlo runs. MEPS-IPNC is compared with LOCSME [14], the modified projection beamformer [7], the reconstruction-estimation based beamformer [13], the beamformer in [29], the beamformer in [16] and the beamformer in [18]. The angular sector of the desired signal is set to be $\Theta = [\bar{\theta}_s - 6^\circ, \bar{\theta}_s + 6^\circ]$ where the interference angular sector is $\bar{\Theta} = [-90^\circ, \bar{\theta}_s - 6^\circ] \cup (\bar{\theta}_s + 6^\circ, 90^\circ]$ and the bound for the beamformer in [18] is set as $\epsilon = \sqrt{0.1}$.

A. Performance of Power Spectrum

We consider a scenario in which the SNR is fixed at -5 dB. Fig. 1 compares the power spectrum of Capon and MEPS methods versus the DoA of the signals. It can be seen that MEPS can effectively retain the power of SOI as well as maintain those of interferences. In fact, high resolution of MEPS comes from extrapolating the partially known autocorrelation function, $r_x(k)$, beyond the last known lag value in a manner that maximizes the entropy of the corresponding power spectrum at each step of the extrapolation [30]. Excellent power spectrum estimates are obtained from relatively short time series data record lengths.

B. Random Signal Look Direction mismatch

In the first example, the impact of random signal look direction mismatch is considered. We assume that the random direction mismatches of the desired signal and the interferers are uniformly distributed in $[-6^\circ, 6^\circ]$. This means that

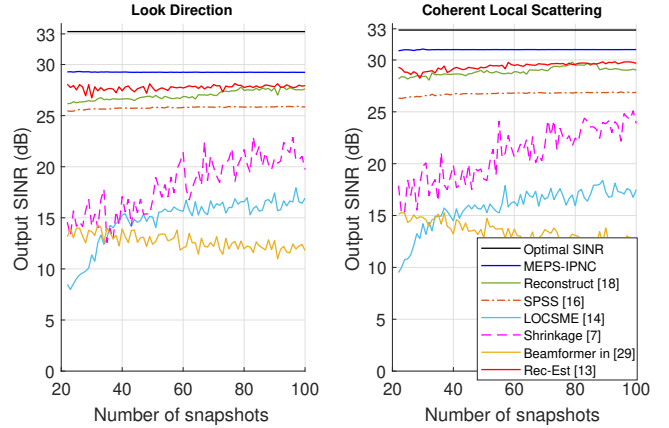


Fig. 3. SINR vs Snapshots a) Look Direction b) Coherent Local Scattering

the actual SOI DoA is uniformly distributed in $[-3^\circ, 9^\circ]$, and the DoAs of the interferers are uniformly distributed in $[-26^\circ, -14^\circ]$ and $[9^\circ, 21^\circ]$. Note that the DoAs of the desired signal and interferences change from run to run while remaining constant over samples. Figs. 2(a) and 3(a) illustrate the SINR performance versus the SNR and snapshots under the look direction case. MEPS-IPNC almost attains the optimal output SINR in both low and high SNRs even when there exist large look direction mismatches, already with only $K = 22$ snapshots. The excellent performance of MEPS-IPNC derives from its high accuracy estimate of the IPNC matrix and the SV of the SOI, which enhance the robustness of MEPS-IPNC against random look direction errors for all numbers of snapshots. MEPS-IPNC outperforms the others and is close to the optimum SINR, with very low variance.

C. Effect of the Coherent Local Scattering errors

In this scenario, the impact of the desired signal SV mismatch due to coherent local scattering [31] on array output SINR is considered. In this example, the presumed signal is a plane wave impinging from $\bar{\theta}_s = 3^\circ$, whereas the actual spatial signature is formed by five signal paths as $\bar{\mathbf{a}} = \bar{\mathbf{a}} + \sum_{i=1}^4 e^{j\varphi_i} \mathbf{d}(\theta_i)$, where $\bar{\mathbf{a}}$ is the direct path and corresponds to the assumed signal SV, and $\mathbf{d}(\theta_i)$ represents the i th coherently scattered path with the direction $\theta_i, (i=1,2,3,4)$ which are randomly distributed in a Gaussian distribution with mean $\bar{\theta}_s$ and standard deviation 2° . Also, the parameters φ_i denote the path phases which are drawn uniformly from the interval $[0, 2\pi]$ in each simulation run. Note that θ_i and $\varphi_i (i=1,2,3,4)$ only change from run to run while remaining fixed from snapshot to snapshot. Figs. 2(b) and 3(b) depict the SINR performance versus SNR and snapshots. Compared to the look direction results, MEPS-IPNC is able to outperform the remaining robust beamformers over a range of snapshots and with less fluctuation in the estimates. The reason for this performance is the combined use of accurate estimates of the IPNC matrix and of the steering vector mismatch.

V. CONCLUSION

In this letter, a new low-complexity approach to RAB is proposed based on highly accurate estimation of the IPNC matrix and the actual SV using MEPS. Simulations demonstrate that the proposed algorithm outperforms some of the recent methods in the literature.

REFERENCES

- [1] H. L. Van Trees, *Detection, Estimation, and Modulation Theory*. John Wiley & Sons, New York, 2004.
- [2] S. Shahbazpanahi, A. B. Gershman, Z.-Q. Luo, and K. M. Wong, "Robust adaptive beamforming for general-rank signal models," *IEEE Trans. on Signal Process.*, vol. 51, no. 9, pp. 2257–2269, 2003.
- [3] J. Li, P. Stoica, and Z. Wang, "On robust Capon beamforming and diagonal loading," *IEEE Trans. on Signal Process.*, vol. 51, no. 7, pp. 1702–1715, 2003.
- [4] L. Zhang and W. Liu, "Robust forward backward based beamformer for a general-rank signal model with real-valued implementation," *Signal Process.*, vol. 92, no. 1, pp. 163–169, 2012.
- [5] X. Mestre and M. A. Lagunas, "Finite sample size effect on minimum variance beamformers: Optimum diagonal loading factor for large arrays," *IEEE Trans. on Signal Process.*, vol. 54, no. 1, pp. 69–82, 2006.
- [6] S. Mohammadzadeh and O. Kukrer, "Modified robust Capon beamforming with approximate orthogonal projection onto the signal-plus-interference subspace," *Circuits, Systems, and Signal Process.*, pp. 1–18, 2018.
- [7] F. Huang, W. Sheng, and X. Ma, "Modified projection approach for robust adaptive array beamforming," *Signal Process.*, vol. 92, no. 7, pp. 1758–1763, 2012.
- [8] W. Jia, W. Jin, S. Zhou, and M. Yao, "Robust adaptive beamforming based on a new steering vector estimation algorithm," *Signal Processing*, vol. 93, no. 9, pp. 2539–2542, 2013.
- [9] S. A. Vorobyov, A. B. Gershman, and Z.-Q. Luo, "Robust adaptive beamforming using worst-case performance optimization: A solution to the signal mismatch problem," *IEEE Trans. on Signal Process.*, vol. 51, no. 2, pp. 313–324, 2003.
- [10] S. E. Nai, W. Ser, Z. L. Yu, and H. Chen, "Iterative robust minimum variance beamforming," *IEEE Trans. on Signal Process.*, vol. 59, no. 4, pp. 1601–1611, 2011.
- [11] A. Khabbazibasmenj, S. A. Vorobyov, and A. Hassanien, "Robust adaptive beamforming via estimating steering vector based on semidefinite relaxation," in *Signals, Systems and Computers (ASILOMAR), 2010 Conference Record of the Forty Fourth Asilomar Conference on*. IEEE, 2010, pp. 1102–1106.
- [12] A. Hassanien, S. A. Vorobyov, and K. M. Wong, "Robust adaptive beamforming using sequential quadratic programming: An iterative solution to the mismatch problem," *IEEE Signal Process. Lett.*, vol. 15, pp. 733–736, 2008.
- [13] Y. Gu and A. Leshem, "Robust adaptive beamforming based on interference covariance matrix reconstruction and steering vector estimation," *IEEE Trans. on Signal Process.*, vol. 60, no. 7, pp. 3881–3885, 2012.
- [14] H. Ruan and R. C. de Lamare, "Robust adaptive beamforming using a low-complexity shrinkage-based mismatch estimation algorithm," *IEEE Signal Process. Lett.*, vol. 21, no. 1, pp. 60–64, 2014.
- [15] X. Yuan and L. Gan, "Robust algorithm against large look direction error for interference-plus-noise covariance matrix reconstruction," *Electronics Letters*, vol. 52, no. 6, pp. 448–450, 2016.
- [16] Z. Zhang, W. Liu, W. Leng, A. Wang, and H. Shi, "Interference-plus-noise covariance matrix reconstruction via spatial power spectrum sampling for robust adaptive beamforming," *IEEE Signal Processing Letters*, vol. 23, no. 1, pp. 121–125, 2016.
- [17] L. Huang, J. Zhang, X. Xu, and Z. Ye, "Robust adaptive beamforming with a novel interference-plus-noise covariance matrix reconstruction method," *IEEE Trans. Signal Process.*, vol. 63, no. 7, pp. 1643–1650, 2015.
- [18] Z. Zheng, Y. Zheng, W.-Q. Wang, and H. Zhang, "Covariance matrix reconstruction with interference steering vector and power estimation for robust adaptive beamforming," *IEEE Transactions on Vehicular Technology*, vol. 67, no. 9, pp. 8495–8503, 2018.
- [19] S. Mohammadzadeh and O. Kukrer, "Adaptive beamforming based on theoretical interference-plus-noise covariance and direction-of-arrival estimation," *IET Signal Process.*, vol. 12, no. 7, pp. 819–825, 2018.
- [20] H. Ruan and R. C. de Lamare, "Robust adaptive beamforming based on low-rank and cross-correlation techniques," *IEEE Transactions on Signal Processing*, vol. 64, no. 15, pp. 3919–3932, Aug 2016.
- [21] S. D. Somasundaram and A. Jakobsson, "Degradation of covariance reconstruction-based robust adaptive beamformers," in *Sensor Signal Process. for Defence (SSPD), 2014*. IEEE, 2014, pp. 1–5.
- [22] Y. Wang, Q. Bao, and Z. Chen, "Robust adaptive beamforming using iaa-based interference-plus-noise covariance matrix reconstruction," *Electronics Letters*, vol. 52, no. 13, pp. 1185–1186, 2016.
- [23] R. T. Lacoss, "Data adaptive spectral analysis methods," *Geophysics*, vol. 36, no. 4, pp. 661–675, 1971.
- [24] T. M. Cover and J. A. Thomas, *Elements of information theory*. John Wiley & Sons, 1991.
- [25] G. T. Wilson, "A convergence theorem for spectral factorization," *Journal of Multivariate Analysis*, vol. 8, no. 2, pp. 222–232, 1978.
- [26] M. H. Hayes, *Statistical digital signal processing and modeling*. John Wiley & Sons, 2009.
- [27] J. Capon, "High-resolution frequency-wavenumber spectrum analysis," *Proceedings of the IEEE*, vol. 57, no. 8, pp. 1408–1418, 1969.
- [28] G. H. Golub and C. F. V. Loan, *Matrix Computations*, 3rd ed. Johns Hopkins, 1996.
- [29] A. Khabbazibasmenj, S. A. Vorobyov, and A. Hassanien, "Robust adaptive beamforming based on steering vector estimation with as little as possible prior information," *IEEE Trans. on Signal Process.*, vol. 60, no. 6, pp. 2974–2987, 2012.
- [30] A. van den Bos, "Alternative interpretation of maximum entropy spectral analysis (corresp.)," *IEEE Trans. on Information Theory*, vol. 17, no. 4, pp. 493–494, 1971.
- [31] J. Goldberg and H. Messer, "Inherent limitations in the localization of a coherently scattered source," *IEEE Trans. on Signal Process.*, vol. 46, no. 12, pp. 3441–3444, 1998.